


Nucleotide-binding oligomerization domain protein 2 deficiency enhances CHOP expression and plaque necrosis in advanced atherosclerotic lesions

Min-Young Kwon^{1,2}, Narae Hwang¹, Sung Hoon Back¹, Seon-Jin Lee³, Mark A. Perrella² and Su Wol Chung¹ 

1 Laboratory of Molecular Immunology, Department of Biological Sciences, University of Ulsan, South Korea

2 Division of Pulmonary and Critical Care Medicine, Brigham and Women's Hospital and Harvard Medical School, Boston, MA, USA

3 Environmental Disease Research Center, KRIBB, Daejeon, Korea

Keywords

ATF6; cell death; CHOP; ER stress; NOD2

Correspondence

S. W. Chung, Laboratory of Molecular Immunology, School of Biological Sciences, University of Ulsan, 93 Daehak-ro, Nam-gu, Ulsan 44610, South Korea
Tel: +82 52 259 1641
E-mail: swchung@ulsan.ac.kr

(Received 10 September 2019, revised 4 February 2020, accepted 11 March 2020)

doi:10.1111/febs.15294

Endoplasmic reticulum (ER) stress-induced cell death of vascular smooth muscle cells (VSMCs) is extensively involved in atherosclerotic plaque stabilization. We previously reported that nucleotide-binding oligomerization domain protein 2 (NOD2) participated in vascular homeostasis and tissue injury. However, the role and underlying mechanisms of NOD2 remain unknown in ER stress-induced cell death of VSMC during vascular diseases, including advanced atherosclerosis. Here, we report that NOD2 specifically interacted with ER stress sensor activating transcription factor 6 (ATF6) and suppressed the expression of proapoptotic transcription factor CHOP (C/EBP homologous protein) during ER stress. CHOP-positive cells were increased in neointimal lesions after femoral artery injury in NOD2-deficient mice. In particular, a NOD2 ligand, MDP, and overexpression of NOD2 decreased CHOP expression in wild-type VSMCs. NOD2 interacted with an ER stress sensor molecule, ATF6, and acted as a negative regulator for ATF6 activation and its downstream target molecule, CHOP, that regulates ER stress-induced apoptosis. Moreover, NOD2 deficiency promoted disruption of advanced atherosclerotic lesions and CHOP expression in NOD2^{-/-}ApoE^{-/-} mice. Our findings indicate an unsuspected critical role for NOD2 in ER stress-induced cell death.

Introduction

Atherosclerosis is a vascular disease featured by atheromatous plaques in the intima of medium and large size arteries, and is the major cause of death among adulthoods in the developed country [1]. An advanced plaque consists of a fibrous cap overlying a lipid mass, called the necrotic core [1]. The fibrous cap is consisted primarily of VSMCs and a comparatively dense extracellular matrix made of elastin, proteoglycans, and collagen. The cell death of VSMCs within

the plaque may imperil the lesion owing to decreased collagen production, consequently thinning the protective fibrous cap, and causing accumulation of cell debris, in addition to intense intimal inflammation [2]. Moreover, VSMC cell death itself is adequate to induce features of plaque vulnerability in atherosclerosis [2,3].

Most importantly, animal models of atherosclerosis and analysis of human atherosclerotic lesions have

Abbreviations

ATF6, activating transcription factor 6; CHOP, transcription factor C/EBP homologous protein; ER stress, endoplasmic reticulum stress; ERSE, cis-acting ER stress response element; IRE1, inositol requiring protein 1; LRRs, leucine-rich repeats; MDP, muramyl dipeptide; NOD2, nucleotide-binding oligomerization domain protein 2; PERK, protein kinase RNA-like endoplasmic reticulum kinase; PRRs, pattern recognition receptors; TLRs, toll-like receptors; VSMCs, vascular smooth muscle cells; XBP1, X-box binding protein 1.

shown obvious evidence that ER stress induces in atherosclerotic plaques, especially in the advanced stage of atherosclerosis [4]. Various inducers of ER stress have been identified, including increased CHOP (C/EBP homologous protein) levels in VSMCs following mechanical stretch, or in the presence of homocysteine, 7-ketocholesterol, unesterified cholesterol, or glucosamine [5]. The expression of CHOP is mainly regulated by three factors, PERK (protein kinase RNA-like endoplasmic reticulum kinase)/ATF4, ATF6 (activating transcription factor 6), and IRE-1 (inositol requiring protein 1)/XBP1 [6]. ER stress-induced CHOP expression plays a critical role in cell death *in vitro* and *in vivo* [7]. However, more work is needed to investigate the mechanisms of ER stress-induced CHOP expression in VSMCs.

Nucleotide-binding oligomerization domain protein 2, initially described as a susceptibility gene for inflammatory bowel diseases such as Crohn's disease, is an intracellular protein LRRs (containing leucine-rich repeats) similar to those found in TLRs (Toll-like receptors) [8]. As an intracellular PRR (pathogen recognition receptor), NOD2 perceives bacterial peptidoglycans from gram-positive and gram-negative bacteria, through its interaction with MDP (muramyl dipeptide) [9,10]. NOD2 is widely expressed in dendritic cells, macrophages, and at lower levels in intestinal epithelial cells and VSMCs [11]. In cultured intestinal epithelial cells, NOD2 expression can be induced by the proinflammatory cytokines TNF- α and IFN- γ [12]. In addition to NOD2 as a PRR, novel functions of NOD2 have been suggested for other cell types, such as adipocytes, gingival and pulp fibroblasts, and vascular endothelial cells [13]. In particular, studies examining the role of NOD2 in vasculatures have revealed that NOD2-mediated signaling pathways and expression have a protective role in vascular homeostasis and tissue injury, and that NOD2 is involved in the regulation of proliferation and differentiation of vascular smooth muscle cells [14]. Previously, we demonstrated the protective effects of NOD2 in a vascular injury model of neointimal hyperplasia [15]. Recently, we published that ER stress-induced cell death was enhanced in NOD2-deficient VSMCs, and that this phenomenon was reversed in NOD2 overexpressed VSMCs. However, the role of NOD2 in the formation of necrotic cores in advanced atherosclerosis, and the molecular mechanisms of NOD2 during ER stress are not known. In this study, we found that NOD2 could regulate ER stress-induced CHOP expression and elucidated the molecular mechanisms of its regulation in VSMCs.

Results

NOD2 deficiency induces CHOP expression in VSMCs after vascular injury

ER stress is a character of advanced or progressed vascular diseases, including atherosclerosis [16]. Prior studies have determined that functional NOD2 is expressed in VSMCs, and VSMC proliferation, migration, and neointimal formation were promoted in NOD2-deficient VSMCs after femoral artery injury [15]. In particular, an absence of NOD2 was found to increase the intimal/media ratio 2.86-fold in NOD2^{-/-} compared with NOD2^{+/+} mice after femoral artery injury [15]. In this study, we hypothesized that NOD2 was associated with ER stress in VSMCs and contributes to the progression of neointimal formation after femoral artery injury. To investigate the role of NOD2 in vasculature, the expression of CHOP in femoral arteries of NOD2^{+/+} and NOD2^{-/-} mice, of similar neointimal size, was examined after femoral artery injury. After immunohistochemistry staining for CHOP, morphometric analysis demonstrated that the number of CHOP-positive cells was significantly higher in NOD2^{-/-} neointima than NOD2^{+/+} neointima of the same size, in femoral artery injury-induced neointima (Fig. 1A,B). There were no significant differences in CHOP expression in noninjured femoral arteries between NOD2^{+/+} and NOD2^{-/-} mice. In NOD2^{+/+} and NOD2^{-/-} VSMCs, mRNA and protein levels of CHOP were analyzed by quantitative real-time RT-PCR or western blotting after administration of tunicamycin, an ER stress inducer. mRNA and protein levels of CHOP were significantly increased by tunicamycin in NOD2^{-/-} VSMCs (Fig. 1C,D). However, other ER stress-induced cell death pathways, including JNK (c-Jun N-terminal kinase) and caspase-12, were not enhanced in NOD2^{-/-} VSMCs tunicamycin, compared with NOD2^{+/+} VSMCs (Fig. 1F,G). We confirmed that mRNA levels of NOD2 were increased in response to tunicamycin-induced ER stress (Fig. 1E). To determine how NOD2 is activated to suppress ER stress-induced CHOP expression, we examined CHOP expression in the presence of NOD2 ligand, MDP. Vehicle, tunicamycin, or tunicamycin plus MDP were injected into mouse peritoneum, and total protein was harvested from the aorta 24 h postinjection. Protein levels of CHOP were analyzed by western blotting. The NOD2 ligand, MDP, decreased tunicamycin-induced CHOP expression in mouse aorta (Fig. 2A). To confirm the effects of NOD2 ligand on suppression of CHOP expression, we treated VSMCs with vehicle, tunicamycin, palmitic acid, tunicamycin plus MDP, or

PA (palmitic acid) plus MDP, and analyzed protein levels of CHOP (Fig. 2B,C). Palmitic acid is a well-known atherogenic factor and ER stress inducer [17]. The NOD2 ligand, MDP, decreased tunicamycin and palmitic acid-induced CHOP protein levels in VSMCs. When mRNA levels of CHOP were examined at 6, 12, and 24 h after vehicle, tunicamycin, or tunicamycin plus MDP treatment in VSMCs (Fig. 2D), MDP was found to decrease mRNA levels of CHOP in NOD2^{+/+} VSMCs. To substantiate the downregulation of NOD2 in ER stress-induced CHOP expression, we examined whether overexpression of NOD2 would exhibit a negative effect on CHOP expression. Control vector (pcDNA3/Flag-GFP) or NOD2 expression vector (pcDNA3/Flag-NOD2) was transfected, and control vector or mouse NOD2-expressing cells were selected with neomycin selectable marker in NOD2^{+/+} VSMCs. The cells were treated with tunicamycin for various times, and proteins levels and mRNA were examined by western blotting and quantitative real-time RT-PCR, respectively. Expression levels of CHOP protein (Fig. 2E) and mRNA (Fig. 2F) were downregulated in the presence of mouse NOD2 overexpression. Furthermore, tunicamycin-induced CHOP expression was decreased by NOD2 overexpression in NOD2^{-/-} VSMCs (data not shown). The overexpression of control vector and mouse NOD2 was determined using Flag antibody (Fig. 2G). On the other hand, the NOD1 and TLR2 ligands, iE-DAP (D- γ -glu-mDAP) and PGN (peptidoglycan), respectively, had no effects or even slightly enhanced on tunicamycin-induced CHOP expression in VSMCs (Fig. 2H,I). In fact, PGN was even found to increase tunicamycin-induced CHOP expression. These data suggest that NOD2 plays a key role in the suppression of CHOP expression in VSMCs after vascular injury.

Interaction between NOD2 and ATF6 represses CHOP promoter activity

Based on the above findings, we studied the CHOP promoter (-870/+24) fused to the firefly luciferase gene using transient transfection assays. The full-length promoter showed to tunicamycin treatment by enhancing luciferase expression approximately 2.7-fold (Fig. 3A). Deletion of the -870 to -160 regions significantly reduced basal expression and increased inducibility up to approximately 8.6-fold. Interestingly, full-length (-870/+24) and deletion (-160/+24) promoter activities were decreased in the presence of NOD2. However, further deletion from -160 to -50 completely abolished the induction by tunicamycin and response to NOD2 (Fig. 3A). This indispensable region from -160 to -50 contains the ERSE (cis-acting

ER stress response element) 1 and ERSE2 sites, which are binding sites for ATF6 and XBP1 (X-box binding protein 1) [18]. To determine whether NOD2 decreases CHOP promoter activity through interaction with ATF6 or XBP1, CHOP (-160/+24) promoter construct was cotransfected with or without NOD2 in wild-type, XBP1^{-/-}, or ATF6^{-/-} MEF cells. The cells were treated with tunicamycin 16 h after transfection and promoter activity was analyzed. Cotransfected NOD2 suppressed the activity of tunicamycin-induced CHOP (-160/+24) promoter activity in wild-type and XBP1^{-/-} MEF cells (Fig. 3B). However, the suppressive effects of NOD2 on CHOP (-160/+24) promoter activity were not present in ATF6^{-/-} MEF cells (Fig. 3B). mRNA expression of XBP1s, splice form, or ATF6 was identified from wild-type, XBP1^{-/-}, or ATF6^{-/-} MEF cells after vehicle or tunicamycin administration (Fig. 3C,D). To determine whether NOD2 decreases transcriptional activity of ATF6, we generated an ERSE1/2 mutant containing the CHOP (-160/+24) ERSE1/2m promoter construct. CHOP (-160/+24) ERSE1/2 and ERSE1/2m were transfected with vehicle or ATF6 with or without NOD2, and promoter activity was analyzed (Fig. 3E). ATF6 increased CHOP (-160/+24) ERSE1/2 promoter activity 4.7-fold compared to the vehicle control. Additionally, NOD2 suppressed ATF6-induced CHOP (-160/+24) ERSE1/2 promoter activity. However, CHOP (-160/+24) ERSE1/2m promoter activity showed very low basal activity and abolished ATF6 induction and response to NOD2 (Fig. 3E). To verify that CHOP (-160/+24) ERSE1/2 sites are important regions for NOD2-mediated suppression of CHOP expression, we generated CHOP (-160/-62), ERSE1/2, and CHOP (-160/-62) ERSE1/2m minimal promoter constructs. To construct the CHOP-ERSE1/2 and CHOP-ERSE1/2m minimal promoter, CHOP-ERSE1/2 (-160 to -62) and CHOP-ERSE1/2m within the -160 to -62 promoter region were inserted into the beginning of the SV40 promoter. CHOP-ERSE1/2 minimal promoter showed a lower response to ATF6 than the CHOP-ERSE1/2 (-160/+24) promoter (Fig. 3F). Nevertheless, this experiment confirmed that NOD2 downregulates CHOP transcriptional activity through ERSE1/2 sites. These data suggest that NOD2 is an important suppressor of ERSE-mediated induction of CHOP expression triggered by tunicamycin-induced ER stress.

Card2 domain of NOD2 interacts with ATF6 during ER stress

Although NOD2 downregulated ATF6-mediated CHOP promoter activity, the expression of phospho-PERK and phospho-IRE1 α and cleaved ATF6

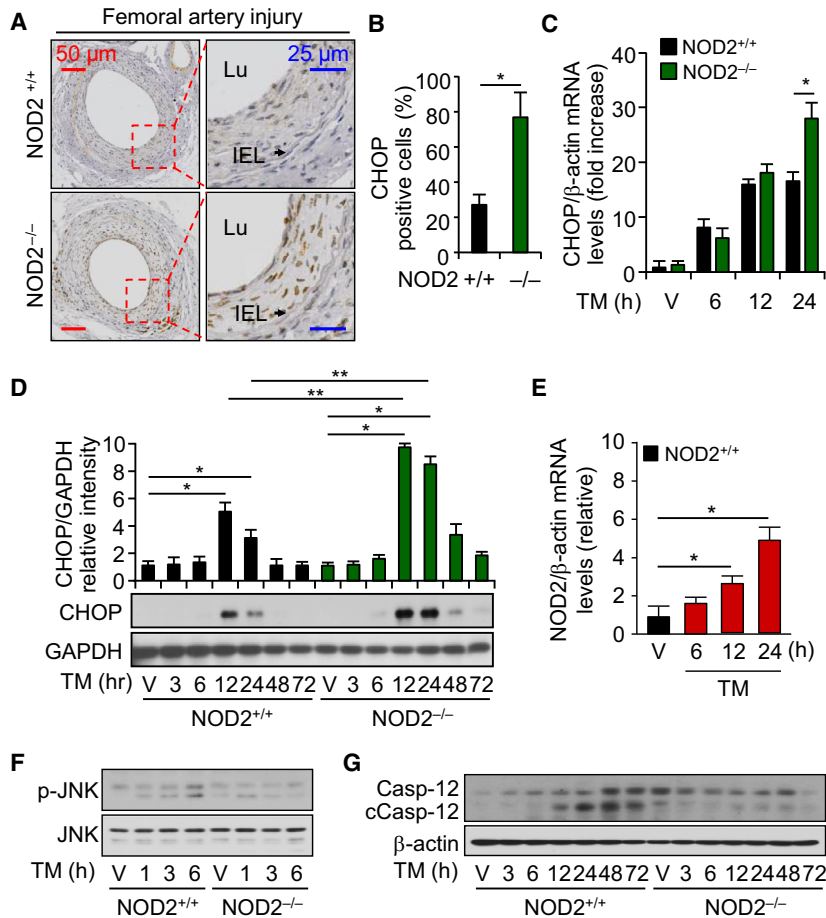


Fig. 1. Nucleotide-binding oligomerization domain-containing protein 2 (NOD2) deficiency induces CHOP (C/EBP homologous protein) expression after vascular injury in mice. (A) Femoral arteries were harvested 28 days after injury. The immunostaining for CHOP was performed on sections from NOD2^{+/+} and NOD2^{-/-} mice. Arrows indicate IEL (internal elastic lamina) of the vessels. Lu represents the vessel lumen. (B) CHOP-positive cells were counted in NOD2^{+/+} (*n* = 10) and NOD2^{-/-} (*n* = 16) vessels after injury. Student's two-tailed unpaired *t*-test, **P* < 0.05, NOD2^{+/+} vs NOD2^{-/-}. Data are represented as mean \pm SD. (C) Quantitative real-time RT-PCR was performed to assess mRNA levels of CHOP in NOD2^{+/+} and NOD2^{-/-} VSMCs 6, 12, and 24 h after vehicle (V) or tunicamycin (100 ng·mL⁻¹) treatment. Mann-Whitney *U*-test, **P* < 0.05, upregulation of gene expression in NOD2^{-/-} vs NOD2^{+/+} VSMCs. For all real-time PCR analyses, mouse β -actin was used as a control for normalization. Values are mean \pm SD, with *n* = 3. (D) Western blotting for CHOP was performed 3, 6, 12, 24, 48, or 72 h after vehicle (V) or tunicamycin administration in NOD2^{-/-} vs NOD2^{+/+} VSMCs. GAPDH (glyceraldehyde-3-phosphate dehydrogenase) was used as a control for normalization. Mann-Whitney *U*-test, **P* < 0.05, upregulation of CHOP expression in tunicamycin vs vehicle, ***P* < 0.05, upregulation of CHOP expression in NOD2^{-/-} vs NOD2^{+/+} VSMCs. Values are mean \pm SD, *n* = 3. (E) Total RNA was extracted from VSMCs at various points, 6, 12, 24 h after tunicamycin administration. The mRNA levels of NOD2 were analyzed by quantitative real-time RT-PCR. For all of the real-time RT-PCR analyses, mouse β -actin was used as controls for normalization. Mann-Whitney *U*-test, **P* < 0.05, upregulation of NOD2 expression in tunicamycin vs vehicle. Values are mean \pm SD, *n* = 3. Vehicle and tunicamycin were treated in NOD2^{+/+} and NOD2^{-/-} VSMCs. Total protein was harvested after treatment at various time points. JNK (c-Jun N-terminal kinases) and phosphorylated JNK (F) and caspase-12, cleaved caspase-12 (G) were assessed by western blot analysis. β -actin was used as controls for normalization. NOD2^{+/+} is in black square and NOD2^{-/-} is in dark green square.

(ATF6p) was similar between NOD2^{+/+} and NOD2^{-/-} VSMCs in the presence of tunicamycin (data not shown). Furthermore, the expression of cleaved ATF6 was enhanced in MDP administrated and NOD2 over-expressed NOD2^{+/+} VSMCs (data not shown). These data suggest that NOD2 may not involve in the

expression and cleavage of ATF6 during tunicamycin-induced ER stress. To investigate the interaction between NOD2 and ATF6 is critical for the suppression of CHOP promoter activity, their interaction was examined. At first, the subcellular localization of NOD2, a NOD2-GFP fusion construct and pDdRed2-

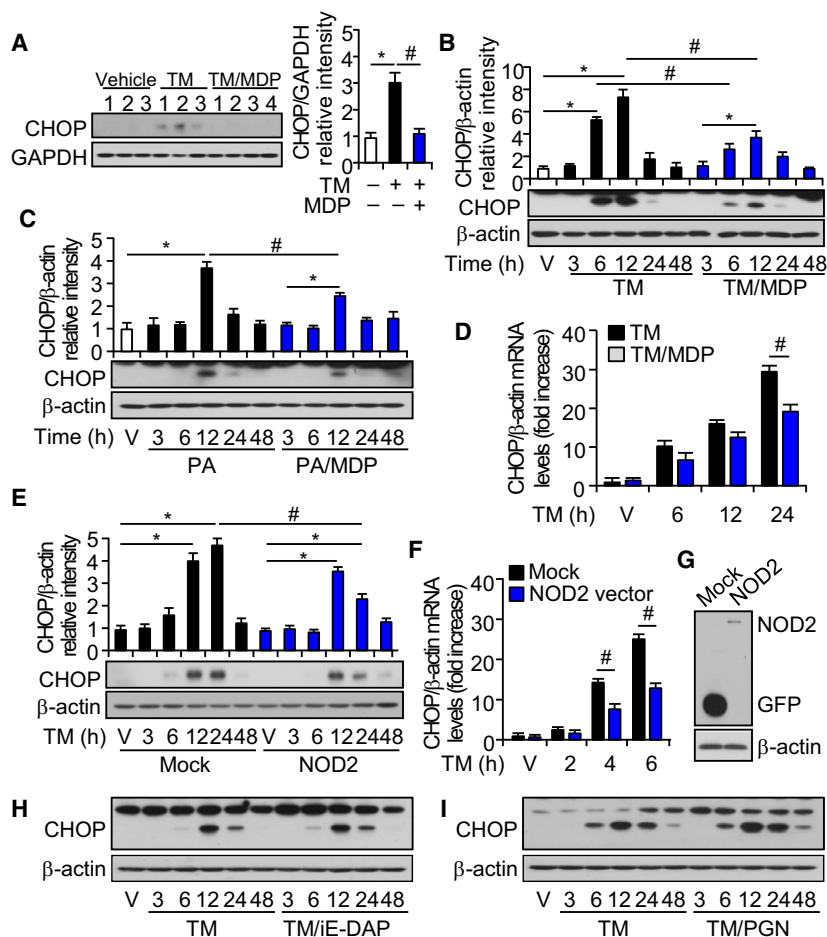


Fig. 2. Nucleotide-binding oligomerization domain protein 2 suppresses ER stress-induced CHOP expression in $NOD2^{+/+}$ VSMCs. (A) Mice were injected with vehicle (0.2% DMSO), TM (tunicamycin 2 mg·kg⁻¹), and TM plus MDP (muramyl dipeptide, 5 mg·kg⁻¹), and aortas were harvested 24 h postinjection. Levels of CHOP protein were analyzed from total cell extracts of aortas. The numbers correspond to individual mice. Mann–Whitney *U*-test, **P* < 0.05, upregulation of CHOP expression in tunicamycin vs vehicle, #*P* < 0.05, downregulation of CHOP expression in tunicamycin plus MDP vs tunicamycin. Values are mean ± SD, *n* = 3. (B) $NOD2^{+/+}$ VSMCs were treated with vehicle (V), TM (100 ng·mL⁻¹), and TM plus MDP (1 μg·mL⁻¹). Levels of CHOP protein were analyzed 3, 6, 12, 24, and 48 h after treatment. Mann–Whitney *U*-test, **P* < 0.05, upregulation of CHOP expression in tunicamycin vs vehicle, #*P* < 0.05, downregulation of CHOP expression in tunicamycin plus MDP vs tunicamycin. Values are mean ± SD, *n* = 3. (C) $NOD2^{+/+}$ VSMCs were treated with vehicle (V), PA (palmitic acid, 500 μg·mL⁻¹), and PA plus MDP (1 μg·mL⁻¹). Levels of CHOP protein were analyzed 3, 6, 12, 24, and 48 h after treatment. GAPDH or β-actin was used as controls for normalization. Each figure represents a representative blot of three independent experiments. Mann–Whitney *U*-test, **P* < 0.05, upregulation of CHOP expression in palmitic acid (PA) vs vehicle, #*P* < 0.05, downregulation of CHOP expression in PA plus MDP vs PA. Values are mean ± SD, *n* = 3. (D) Quantitative real-time RT-PCR was performed to assess mRNA levels of CHOP 6, 12, and 24 h after vehicle (V), TM (100 ng·mL⁻¹), or TM plus MDP (1 μg·mL⁻¹) administration in $NOD2^{+/+}$ VSMCs. Mann–Whitney *U*-test, #*P* < 0.05, downregulation of gene expression in TM plus MDP vs TM. For all real-time PCR analyses, mouse β-actin was used as a control for normalization. Values are mean ± SD, *n* = 3. (E) The control vector (Con, pCDNA3/FLAG-GFP) or NOD (pCDNA3/FLAG-NOD2)-expressing vector were introduced into $NOD2^{+/+}$ VSMCs. Western blotting was performed for CHOP 3, 6, 12, 24, or 48 h after vehicle (V) or TM (100 ng·mL⁻¹) treatment. β-actin was used as a control for normalization. The blot is representative of three independent experiments. Mann–Whitney *U*-test, **P* < 0.05, upregulation of CHOP expression in palmitic acid (PA) vs vehicle, #*P* < 0.05, downregulation of CHOP expression in NOD2 overexpression vs mock. Values are mean ± SD, *n* = 3. (F) Quantitative real-time RT-PCR was performed to assess mRNA levels of CHOP 2, 4, and 6 h after vehicle (V) and TM (100 ng·mL⁻¹) in control or NOD2 overexpressed VSMCs. Mann–Whitney *U*-test, #*P* < 0.05, downregulation of gene expression in NOD2 overexpression vs mock. For all real-time PCR analyses, mouse β-actin was used as a control for normalization. Values are mean ± SD, *n* = 3. (G) NOD2 overexpression was analyzed using Flag antibody. $NOD2^{+/+}$ VSMCs were treated vehicle (V), TM (100 ng·mL⁻¹), and TM plus iE-DAP (D-γ-Glu-mDAP, 1 μg·mL⁻¹) (H) or PGN (peptidoglycan, 1 μg·mL⁻¹) (I). The levels of CHOP protein were analyzed 3, 6, 12, 24, and 48 h after treatment. β-actin was used as controls for normalization. This represents a representative blot of three independent experiments.

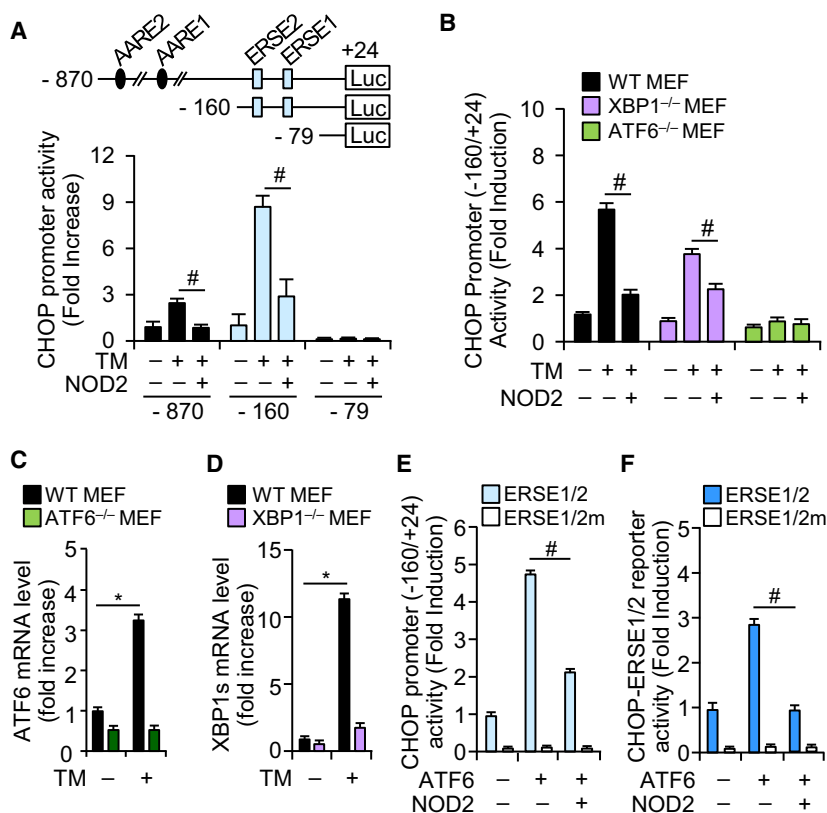


Fig. 3. Nucleotide-binding oligomerization domain protein 2 decreases ER stress-induced CHOP expression through ATF6 (activating transcription factor) and ERSE1 and 2 (ER stress response elements 1 and 2). (A) Various fragments derived from the mouse CHOP promoter regions, $-870/+24$, $-160/+24$, and $-79/+24$, are shown schematically on the top. The numbers indicate nucleotide position from the transcription start site. White ovals and black rectangles indicate the location of AARE motifs and ERSE motifs, respectively. Each of these constructs was transiently introduced into NOD2^{+/+} VSMCs with or without NOD2. Relative luciferase activity in transfected cells incubated for 16 h with or without TM ($2 \mu\text{g}\cdot\text{mL}^{-1}$) was determined, and averages from three independent experiments are presented with standard deviations. CHOP promoter activity was calculated as fold induction compared with activity of construct CHOP ($-870/+24$) exposed to vehicle. Student's two-tailed unpaired *t*-test, $\#P < 0.05$, vs activity of CHOP ($-870/+24$), ($-160/+24$), or ($-79/+24$) promoter constructs stimulated with TM ($2 \mu\text{g}\cdot\text{mL}^{-1}$). Values are mean \pm SD, $n = 12$. (B) CHOP ($-160/+24$) promoter construct was transiently transfected into wild-type, XBP1^{-/-}, or ATF6^{-/-} MEF cells with or without NOD2. Relative luciferase activity in transfected cells incubated for 16 h with or without TM ($2 \mu\text{g}\cdot\text{mL}^{-1}$) was determined. CHOP promoter activity was calculated as fold induction compared with activity of construct CHOP ($-160/+24$) exposed to vehicle in wild-type MEF cells. Student's two-tailed unpaired *t*-test, $\#P < 0.05$, vs activity of CHOP ($-160/+24$) promoter constructs stimulated with TM ($2 \mu\text{g}\cdot\text{mL}^{-1}$) in wild-type and XBP1^{-/-} MEF cells. Values are mean \pm SD, $n = 12$. Quantitative real-time RT-PCR was performed to assess mRNA levels of ATF6 (C) or XBP1s (D) 12 h after vehicle (V) or TM ($100 \text{ ng}\cdot\text{mL}^{-1}$) administration in wild-type, XBP1^{-/-}, or ATF6^{-/-} MEF cells. Mann-Whitney *U*-test, $*P < 0.05$, upregulation of gene expression in TM vs vehicle. For all real-time PCR analyses, mouse β -actin was used as a control for normalization. Values are mean \pm SD, $n = 3$. (E) CHOP ($-160/+24$) ERSE1/2 and ERSE1/2m promoter constructs were transiently transfected into VSMCs with or without NOD2 in the absence or presence of ATF6. Relative luciferase activity in transfected cells incubated for 16 h with or without TM ($2 \mu\text{g}\cdot\text{mL}^{-1}$) was determined. CHOP promoter activity was calculated as fold induction compared with the activity of construct CHOP ($-160/+24$) ERSE1/2 exposed to vehicle. Student's two-tailed unpaired *t*-test, $\#P < 0.05$, vs activity of CHOP ($-160/+24$) ERSE1/2 promoter constructs stimulated with TM ($2 \mu\text{g}\cdot\text{mL}^{-1}$) in VSMCs. Values are mean \pm SD, $n = 12$. (F) CHOP ($-98/-79$) ERSE1/2 and CHOP ($-98/-79$) ERSE1/2m minimal promoter constructs were transiently transfected into VSMCs with or without NOD2 in the absence or presence of ATF6. Relative luciferase activity in transfected cells incubated for 16 h with or without TM ($2 \mu\text{g}\cdot\text{mL}^{-1}$) was determined. CHOP ($-98/-79$) ERSE1/2 and CHOP ($-98/-79$) ERSE1/2m minimal promoter activity was calculated as fold induction compared with the activity of construct CHOP ERSE1/2 exposed to vehicle. Student's two-tailed unpaired *t*-test, $\#P < 0.05$, vs activity of CHOP ERSE1/2 promoter constructs stimulated with TM ($2 \mu\text{g}\cdot\text{mL}^{-1}$) in VSMCs. Values are mean \pm SD, $n = 12$.

ER for fluorescent labeling of the ER were transfected into 293F cells. Transfected cells were treated with tunicamycin, and protein trafficking of NOD2 and red

fluorescent protein fusing with ER retention sequence, KDEL, was examined by conjugated fluorescence protein and confocal imaging (Fig. 4A). The confocal

images clearly demonstrated that NOD2 mainly expressed in the cytoplasm, before localizing to the ER in response to an ER stress inducer. These data raised the possibility that NOD2 may interact with ATF6 and other ER stress sensors, such as IRE1 α and PERK. To specify colocalization between NOD2 and ATF6, IRE1 α , and PERK, NOD2-GFP and ARF6-, IRE1 α -, or PERK-RFP fusion constructs were transfected and treated with tunicamycin. Protein trafficking of NOD2, ATF6, IRE1 α , and PERK proteins was examined using conjugated fluorescence proteins and confocal imaging (Fig. 4B). The confocal images showed that NOD2 colocalized with ATF6 in the absence and presence of the ER stress inducer tunicamycin. Interestingly, colocalization between NOD2 and ATF6 was enhanced under ER stress conditions (Fig. 4B). To determine a physical interaction between NOD2 and ATF6, IRE1 α , or PERK, Flag-tagged NOD2 (Flag-NOD2) construct and HA-tagged ATF6 (HA-ATF6), IRE1 α (HA-IRE1 α), or PERK (HA-PERK) were transfected into 293F cells. Flag-tagged GFP (Flag-GFP) was used as a control protein. Transfected cells were treated with tunicamycin and cell lysates were analyzed by immunoprecipitation using anti-Flag antibody, followed by western blotting analysis with anti-HA antibody (Fig. 4C). To confirm the specific interaction between NOD2 and ATF6, cotransfected 293F cells were treated as indicated and cell lysates were by immunoprecipitation using anti-IgG or anti-Flag antibodies, followed by western blotting analysis with anti-HA antibody (Fig. 4D). As shown in Fig. 4C,D, NOD2 interacted with ATF6 in the absence of ER stress. However, the interaction between NOD2 and ATF6 was prolonged and enhanced in the presence of tunicamycin, but this was not the case for NOD2 interaction with IRE1 α or PERK (Fig. 4C).

To better understand the interaction sites between NOD2 and ATF6, various subregions of NOD2 and ATF6 were deleted, and a schematic representation is shown in Fig. 5A,C of NOD2 and ATF6, respectively. The constructs of HA-tagged ATF6 and Flag-tagged NOD2 domain deletion were transfected as indicated, and treated with vehicle or tunicamycin. Cell lysates were analyzed by immunoprecipitation using anti-Flag antibody, followed by western blot analysis with anti-HA antibody. As previously mentioned, NOD2 contains three distinct motifs: two Cards, NBD, and LRR. Flag-tagged proteins containing only Card2 (Flag-Card2), Flag-tagged Card1/2 (Flag-Card/2), and Flag-tagged Δ LRR (LRR region-deleted NOD2, Flag- Δ LRR) were strongly co-immunoprecipitated with HA-tagged ATF6 in the presence of the ER stress

inducer, tunicamycin (Fig. 5B). However, Flag-tagged proteins containing only Card1 (Flag-Card1), NBD (Flag-NBD), or LRR (Flag-LRR) failed to co-immunoprecipitate with HA-ATF6. To determine the region of ATF6 that interacts with NOD2, HA-tagged ATF6 domain-containing constructs were generated from various regions of ATF6 (Fig. 5C). These HA-tagged ATF6 domain-containing constructs were cotransfected with Flag-tagged NOD2 for immunoprecipitation assays. As shown in Fig. 5D, HA-tagged ATF6 (HA-ATF6) and HA-tagged lumen (lumen region of ATF6, HA-Lumen) were strongly co-immunoprecipitated with Flag-tagged NOD2 (Flag-NOD2) in the presence of ER stress. On the contrary, HA-tagged TAD (TAD region of ATF6, HA-TAD) and basic ZIP (basic leucine zipper region of ATF6, HA-bZIP) constructs have been shown to have a weak interaction with Flag-NOD2 (Fig. 5D). To verify the interaction between NOD2 and ATF6 and their specific interacting region, HA-tagged ATF6 domain-containing constructs were cotransfected with the Flag-tagged Card2 domain construct of NOD2. Figure 5E shows that the interaction between the Card2 domain of NOD2 and ATF6 only occurs for the full-length (HA-ATF6) and luminal region (HA-Lumen) of ATF6. These results suggest that NOD2 interacts with ATF6 through binding the region between Card2 of NOD2 and the lumen region of ATF6.

To substantiate the importance of interacting sites between NOD2 and ATF6, NOD2 deletion constructs were examined that exhibit a trans-suppression effects on CHOP promoter activity (Fig. 6A). The CHOP (-160/+24) promoter was cotransfected with NOD2 deletion mutants, and promoter activity was analyzed after tunicamycin or ATF6 stimulation. Interestingly, only the Card2 domain was involved in physical interaction with ATF6; however, the Card1 and NBD domains were necessary for trans-suppression of CHOP (-160/+24) promoter activity (Fig. 6B,C). These data suggest that NOD2 could be a negative regulator for ATF6 through a physical interaction, and that Card1, Card2, and NBD domains are involved in suppression of its activity.

NOD2 deficiency promotes disruption of advanced atherosclerotic lesions and CHOP expression

In vitro studies have indicated ER stress in cell death of macrophages and smooth muscle cells, a process engaged in plaque necrosis during progressed atheromata. NOD2^{+/+}ApoE^{-/-} and NOD2^{-/-}ApoE^{-/-} mice

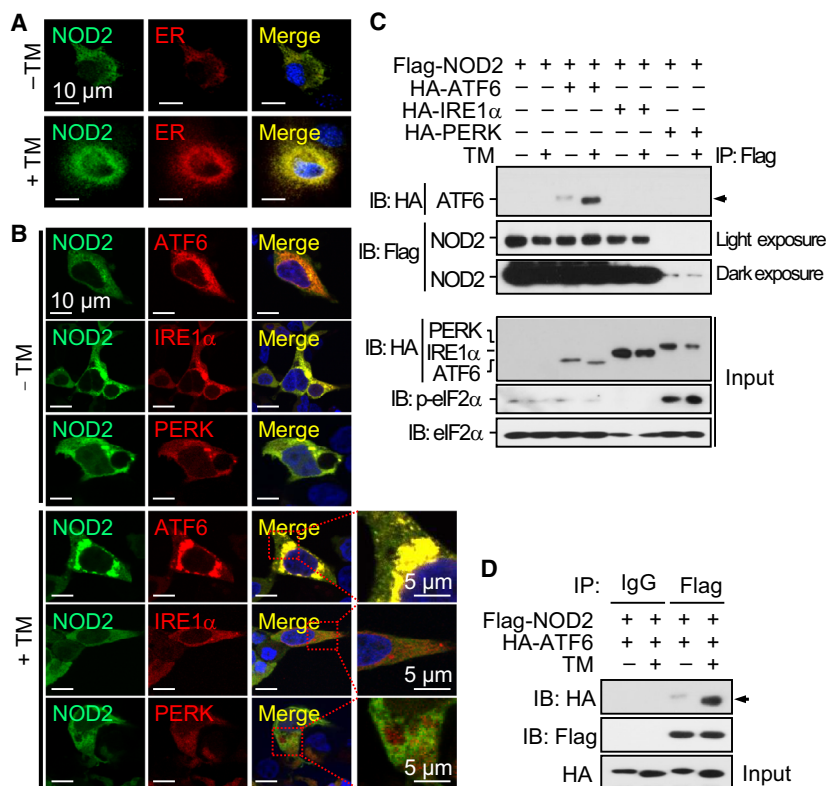


Fig. 4. Nucleotide-binding oligomerization domain protein 2 colocalizes with ATF6 in the ER during ER stress. (A) NOD2-GFP fusion protein (green) and pDsRED-ER (red) were cotransfected in 293F cells and treated with vehicle or tunicamycin for 12 h. Cells were fixed and counterstained with the nuclear dye DAPI (nuclei, blue) before confocal image analysis. Scale bar: 10 μm. (B) The expression construct NOD2-GFP was transiently cotransfected with PERK-RFP, IRE1α-RFP, or ATF6 (full-length)-RFP into 293F cells and treated with vehicle or tunicamycin for 12 h. Immunofluorescence images of DAPI (nuclei, blue), NOD2-GFP (green), PERK-RFP (red), IRE1α-RFP (red), and ATF6 (full-length)-RFP (red). Scale bar: 10 μm. (C) FLAG-NOD2 was co-expressed with HA-PERK, HA-IRE1α, or HA-ATF6 (full-length) in 293F cells as indicated. Flag-NOD2 was co-immunoprecipitated from cell extracts of transfected cells using anti-Flag antibody and immunoblotted with anti-HA antibody. Arrow indicates ATF6 interacting with NOD2. (D) Flag-NOD2 was co-expressed with HA-ATF6 (full-length) in 293F cells as indicated. Flag-NOD2 was co-immunoprecipitated from cell extracts of transfected cells using mouse anti-IgG or anti-Flag antibody, and immunoblotted with anti-HA antibody as a control experiment for Fig. 4C. Arrow indicates ATF6 interacting with NOD2. These data are representative of three individual experiments.

on a C57BL/6 background were placed on an atherogenic diet for 8 or 16 weeks. The mice were then sacrificed and analyzed for lipoprotein, metabolic, and plaque characteristics. To investigate the effect of NOD2 deficiency in animal model of atherosclerosis, ascending aorta of atherogenic diet-fed NOD2^{+/+}ApoE^{-/-} and NOD2^{-/-}ApoE^{-/-} mice were analyzed for morphology and size after being fed a CD (control diet) or AD (atherogenic diet) for 16 weeks, as shown in the representative images in Fig. 7A. Despite of similar plasma lipoproteins, lesion area was 2.65-fold larger in NOD2^{-/-}ApoE^{-/-} mice compared with NOD2^{+/+}ApoE^{-/-} mice (Fig. 7B). In particular, necrotic core size of plaques is an important determinant of plaque vulnerability [19]. Analysis of lesions for acellular nonfibrotic areas revealed an increase in plaque

necrosis in NOD2^{-/-}ApoE^{-/-} mice lesions, and quantification of this parameter for the entire mice cohort indicated a 2.88-fold increase in total necrotic lesion area for NOD2^{-/-}ApoE^{-/-} mice ($P < 0.05$) (Fig. 7C). However, food intake and body weight gain were similar between NOD2^{+/+}ApoE^{-/-} and NOD2^{-/-}ApoE^{-/-} mice after feeding with a normal diet or atherogenic diet for 16 weeks (Fig. 7D,E). To determine CHOP expression in plaques, we analyzed protein levels of CHOP from aorta obtained from mice fed a CD or AD diet for 16 weeks using western blotting analysis (Fig. 7F). Protein levels of CHOP were increased 16 weeks after the start of the AD diet. As expected, protein levels of CHOP were enhanced in aortas of NOD2^{+/+}ApoE^{-/-} and NOD2^{-/-}ApoE^{-/-} mice after feeding with the AD diet. Figure 7F indicates

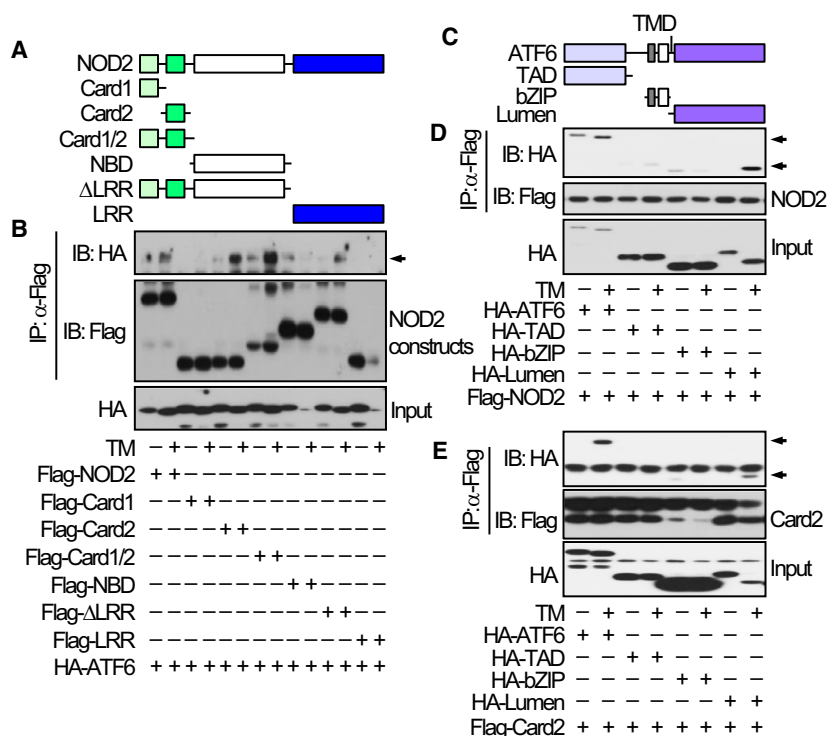


Fig. 5. Nucleotide-binding oligomerization domain protein 2 interacts with a basic leucine zipper (bZip) transcriptional domain of ATF6 through the Card2 domain. (A) Schematic representation of the NOD2 deletion constructs. (B) Flag-tagged NOD2 or deletion constructs were transiently transfected with HA-tagged ATF6 in 293F cells. Flag-tagged NOD2 constructs were immunoprecipitated from cell lysates using anti-Flag antibody. The precipitates were separated by SDS/PAGE and the HA-tagged ATF6 was recognized by immunoblotting with anti-HA antibody. Arrow indicates ATF6 interacting with NOD2 deletion constructs. (C) Schematic representation of the ATF6 deletion constructs. (D) HA-tagged ATF6 or deletion constructs were transiently transfected with Flag-tagged NOD2 in 293F cells. HA-tagged ATF6 constructs were immunoprecipitated from cell lysates using anti-HA antibody. The precipitates were separated by SDS/PAGE and the Flag-tagged NOD2 was recognized by immunoblotting with anti-Flag antibody. Arrows indicate ATF6 deletion constructs interacting with NOD2. (E) Flag-tagged Card2 domain construct of NOD2 was transiently transfected with HA-tagged ATF6 in 293F cells. Flag-tagged Card2 domain construct was immunoprecipitated from cell lysates using anti-Flag antibody. The precipitates were separated by SDS/PAGE and the HA-tagged ATF6 was recognized by immunoblotting with anti-HA antibody. Arrows indicate ATF6 deletion constructs interacting with the Card2 domain construct of NOD2. These data are representative of three individual experiments.

individual mouse number. Importantly, CHOP expression was increased in $NOD2^{-/-}ApoE^{-/-}$ mice compared with $NOD2^{+/+}ApoE^{-/-}$ mice after feeding with an AD diet. To investigate the physiological role of NOD2 in ER stress-induced cell death, we isolated primary aortic VSMCs from $NOD2^{+/+}ApoE^{-/-}$ or $NOD2^{-/-}ApoE^{-/-}$ mice aortas. We then assessed ER stress-induced cell death at various time points after tunicamycin treatment for $NOD2^{+/+}ApoE^{-/-}$ and $NOD2^{-/-}ApoE^{-/-}$ VSMCs. Cell viability of $NOD2^{-/-}ApoE^{-/-}$ (44.88%) VSMCs was decreased 72 h after tunicamycin treatment, compared to $NOD2^{+/+}ApoE^{-/-}$ (67.59%) VSMCs (Fig. 7G). $NOD2^{+/+}ApoE^{-/-}$ and $NOD2^{-/-}ApoE^{-/-}$ mice did not show significantly in total plasma cholesterol, triglyceride, and free fatty acids (Fig. 7H–J). These data indicate that ER stress-induced

CHOP expression of VSMCs may contribute to plaque vulnerability and cell death in $NOD2^{-/-}ApoE^{-/-}$ mice.

Discussion

Atherosclerosis, a silent chronic vascular disease, is the major cause of heart disease and stroke. In developed countries, it is the fundamental cause of ~ 50% of total population deaths [20,21]. The lesion that occurs during atherosclerosis shows a series of highly specific cellular and molecular responses. VSMC proliferation and neointimal formation are important phenomena in the pathophysiological course of atherosclerosis and restenosis after balloon angioplasty [22]. Previously, we demonstrated that NOD2 restrains VSMC proliferation and migration, and prevents neointima

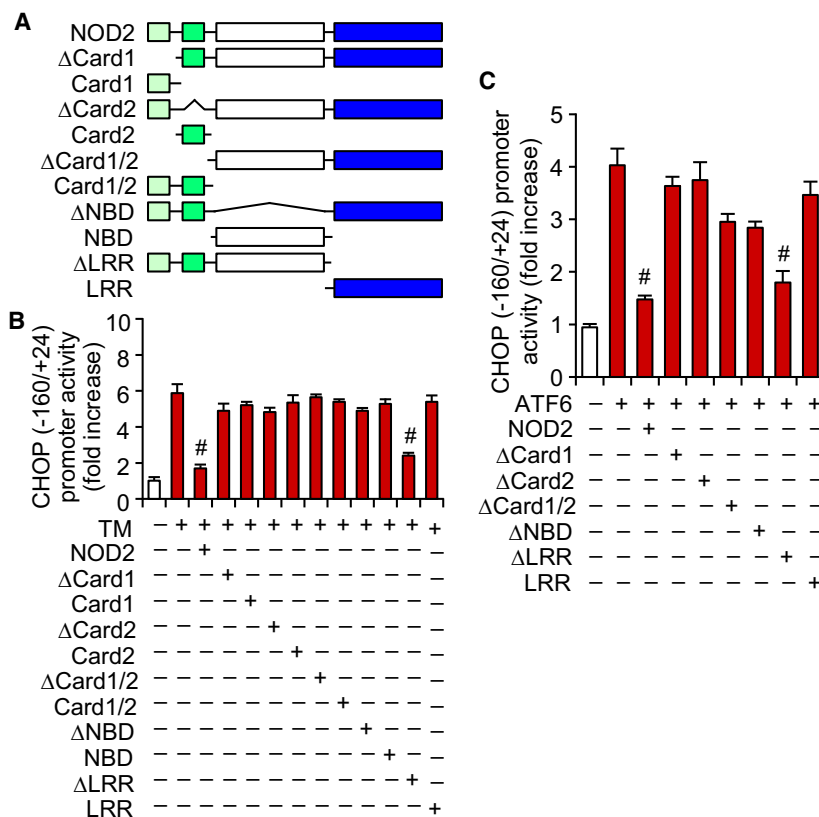


Fig. 6. The Card1, 2, and NBD domains of NOD2 are involved in transrepression of the CHOP promoter. (A) Schematic representation of the NOD2 deletion constructs. (B) The CHOP (-160/+24) construct was transiently transfected with the NOD domain and deletion mutants of NOD2 in VSMCs. Cells were treated with vehicle or TM (2 μ g·mL⁻¹) for 16 h and then harvested for determination of luciferase assay after the transfection. CHOP promoter activity was calculated as fold induction compared with the activity of construct CHOP (-160/+24) exposed to vehicle. Student's two-tailed unpaired *t*-test, #*P* < 0.05, vs. activity of CHOP (-160/+24) in the presence of TM (2 mg·mL⁻¹). Values are mean \pm SD, *n* = 12. (C) CHOP (-160/+24) construct was transiently transfected with NOD2 or NOD2 deletion mutants in the absence or presence of ATF6 (full-length) in VSMCs. CHOP promoter activity was analyzed 16 h after transfection. CHOP promoter activity was calculated as fold induction compared with the activity of construct CHOP (-160/+24) with control plasmid. Student's two-tailed unpaired *t*-test, #*P* < 0.05, vs. activity of CHOP (-160/+24) in the presence of ATF6 (full-length) alone. Values are mean \pm SD, *n* = 12.

formation in a vascular injury model [15]. VSMCs play a key role in regulating plaque stability in advanced atherosclerosis. Once a plaque is established, VSMC death leads to plaque rupture and exposure of pro-thrombotic debris, which can lead to myocardial infarction [23]. Recently, ER stress has been implicated in regulating VSMC phenotype, physiology, and death in vascular diseases [24]. Recent studies show that several atherogenic factors have been identified as ER stress inducers in VSMCs. In the different cell types, CHOP is known as the key molecules for initiating cell death under chronic ER stress [25]. For example, higher CHOP expression due to ER stress is associated with VSMC death in human and mouse studies [26].

In this study, we investigated the hypothesis that NOD2 may have protective effects on ER stress-

induced VSMC death in advanced plaques. We first tested CHOP expression in neointima of NOD2^{+/+} and NOD2^{-/-} vessels after femoral artery injury (Fig. 1A). A significantly higher expression for CHOP was observed in NOD2^{-/-} femoral arteries compared with NOD2^{+/+} femoral arteries. In *in vitro* experiments, the ER stress inducer tunicamycin enhanced expression of CHOP in NOD2^{-/-} VSMCs compared to expression in NOD2^{+/+} VSMCs (Fig. 1C,D). Consistent with these results, we found that NOD2 ligand, MDP, and NOD2 overexpression reduced ER stress-induced CHOP expression in NOD2^{+/+} VSMCs (Fig. 2). Therefore, our data support our initial hypothesis that NOD2 may regulate CHOP expression in VSMCs.

Based on these data, we tested whether NOD2 could regulate CHOP promoter activities and interact with

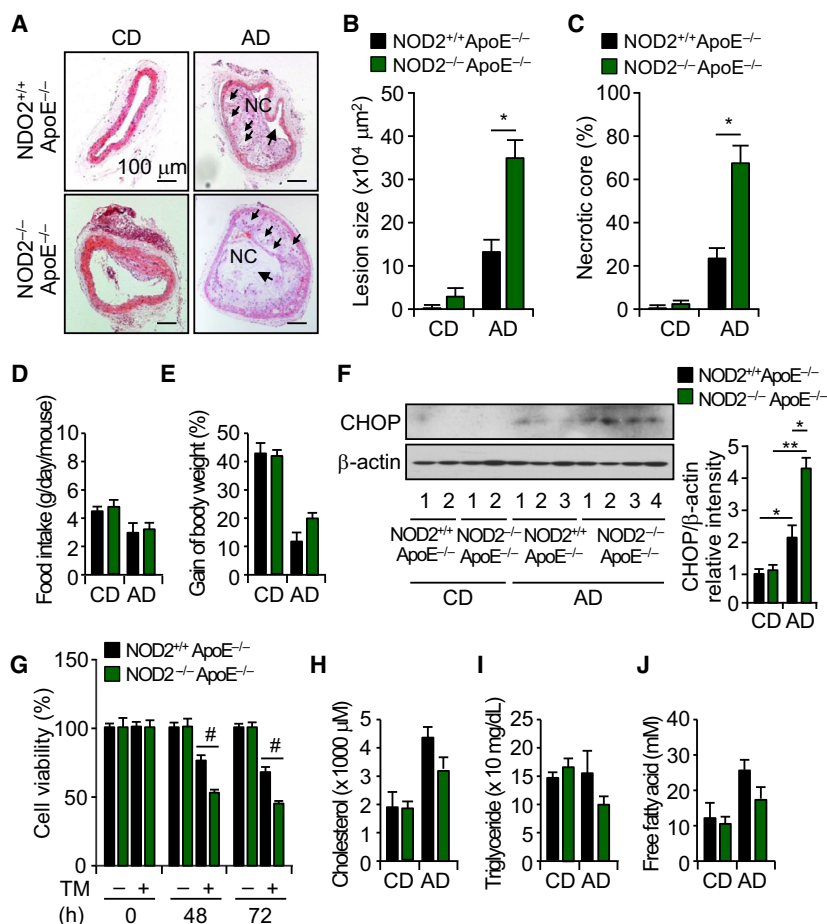


Fig. 7. Nucleotide-binding oligomerization domain protein 2 deficiency promotes disruption of advanced atherosclerotic lesions and CHOP expression. (A) Images show representative sections of ascending aorta from each group of mice stained with hematoxylin and eosin. Quantification was conducted on lesions size (B) and necrotic area in the lesions (C) of NOD2^{+/+}ApoE^{-/-} ($n = 9$) and NOD2^{-/-}ApoE^{-/-} ($n = 12$) mice given control diet or atherogenic diets for 16 weeks. Student's two-tailed unpaired *t*-test, * $P < 0.05$ NOD2^{+/+}ApoE^{-/-} vs NOD2^{-/-}ApoE^{-/-} after administration of an atherogenic diet for 16 weeks. Values are mean \pm SD. Food intake (D) and gain of body weight (E) were monitored twice a week for 16 weeks after CD (control diet) or AD (atherogenic diet) and represented as a graph. Food intake was represented as a gram per day in mouse. Values are mean \pm SD, $n = 9$. NOD2^{+/+}ApoE^{-/-} is in black square and NOD2^{-/-}ApoE^{-/-} is in dark green square. (F) Total protein was harvested from NOD2^{+/+}ApoE^{-/-} and NOD2^{-/-}ApoE^{-/-} mice aortas 16 weeks after the start of either the CD (control diet) or AD (atherogenic diet). Protein levels of CHOP were analyzed using western blotting. The numbers indicate individual mice. Mann-Whitney *U*-test, * $P < 0.05$, upregulation of CHOP expression in AD (atherogenic diet) vs CD (control diet), ** $P < 0.05$, upregulation of CHOP expression in NOD2^{-/-}ApoE^{-/-} vs NOD2^{+/+}ApoE^{-/-} mice aorta. Values are mean \pm SD. (G) Cell viability of NOD2^{+/+}ApoE^{-/-} and NOD2^{-/-}ApoE^{-/-} VSMCs was measured at 0, 48, and 72 h after vehicle or TM (tunicamycin, 100 ng·mL⁻¹) administration using Ez-Cytox Cell Viability Assay Kit. Student's two-tailed unpaired *t*-test, # $P < 0.05$, decreased cell viability of NOD2^{-/-}ApoE^{-/-} vs NOD2^{+/+}ApoE^{-/-} VSMCs in the presence or absence of tunicamycin. Values represent mean \pm SD, $n = 12$. Serum total cholesterol (H), triglyceride (I), and free fatty acid (J) in NOD2^{+/+}ApoE^{-/-} and NOD2^{-/-}ApoE^{-/-} 16 weeks after CD (control diet) or AD (atherogenic diet). Values are mean \pm SD, $n = 9$. NOD2^{+/+}ApoE^{-/-} is in black square and NOD2^{-/-}ApoE^{-/-} is in dark green square.

the ER stress sensors PERK, IRE1, or ATF6, or their downstream targets. Interestingly, NOD2 decreased CHOP promoter activity through interaction with ATF6 at two ERSE sites (Fig. 3). In Fig. 3A, the induction of the CHOP (-870/+24) promoter was much lower than that expected from the induction of CHOP mRNA in the presence of tunicamycin

(Fig. 2F, black bars). However, a high basal activity of the CHOP (-870/+24) promoter, which accounts for its low inducibility, has also been previously reported [27]. Moreover, we found that NOD2 interacted with ATF6 directly, and not with PERK and IRE1 α in the presence of the tunicamycin (Fig. 4). NOD2 interacted weakly with the bZIP transcription

factor domain of ATF6, which is located in the cytosol when tunicamycin is absent (Fig. 4C,D, and Fig. 5B). However, physical interaction of NOD2 and ATF6 was strongly elevated through a Card2 domain of NOD2 and luminal domain of ATF6 in the presence of ER stress inducer, tunicamycin (Fig. 5D,E). Structurally, NOD2 has two caspase recruitment (Card) domains that function as effector domains and mediate specific hemophilic interactions with downstream Card-containing molecules [28]. After activation by the ligand MDP through the LRR (leucine-rich repeat) domain, NOD2 undergoes self-oligomerization and recruitment of the downstream adaptor molecule kinase, RIP2 (receptor interacting protein 2), via a homophilic Card–Card interaction [29]. Active RIP2 induces signaling events and transcription of many genes, including proinflammatory cytokines [30]. NOD2 has also been suggested to play a role in the autophagic process, due to its interaction with autophagy protein ATG16L1 (autophagy Related 16 Like 1), and suppresses inflammatory cytokines through the NOD2 and ATG16L1 signaling axis [31]. We have not yet studied the mechanism by which NOD2 is translocated from the cytosol to the ER lumen in the presence of ER-related stress. However, our data clearly show that the Card2 domain of NOD2 can heterophilically interact with the luminal region of ATF6. Even though the Card2 domain of NOD2 interacted with the luminal region of ATF6, Card2 alone was not sufficient to suppress CHOP promoter activity under ER stress induced by tunicamycin or ATF6. Card1, Card2, and the NBD domain of NOD2, but not the LRR domain, are essential for trans-suppression of NOD2 effects on CHOP promoter ESRE sites through ATF6 (Fig. 6). These data imply that NOD2 can downregulate transcriptional expression of CHOP through ERSE sites in the CHOP promoter region, mediated by NOD2 and ATF6 interaction. Further work should focus on determining whether NOD2 may prevent ATF6 translocation to the nucleus after NOD2 and ATF6 interaction. Recent studies suggest that cytosolic proteins translocate across or insertion into ER membranes using sophisticated transport machinery components such as heterotrimeric Sec61 complexes [32]. In this study, we have not shown the specific molecular mechanisms for NOD2 translocation to ER lumen. Therefore, the mechanism and specific components for NOD2 translocation from cytosol to ER need to be elucidated in the further investigation.

Finally, further work is needed to confirm that NOD2 regulates cell death and prevents necrotic core formation in advanced plaques in an animal

atherosclerosis model. A greater number of necrotic cores were observed in the aortic vessels of NOD2 and ApoE double-deficient mice, compared with NOD2 wild-type and ApoE-deficient mice after an atherogenic diet (Fig. 7). We also confirmed enhanced CHOP expression in the aortas of NOD2 and ApoE double knock-out mice compared with NOD2 wild-type and ApoE knock-out mice after mice were fed an atherogenic diet for 16 weeks. Importantly, NOD2-deficient VSMCs were sensitive to ER stress-induced cell death, compared with normal VSMCs (Fig. 7G). These data confirm that NOD2 can prevent higher expression of CHOP, cell death, and necrotic core formation in advanced plaques of atherosclerosis.

Other studies have examined the role of PRRs, such as TLRs or NLRs (NOD-like receptors), during ER stress in inflammatory or vascular diseases [29]. TLRs are thought to mediate macrophage cell death and plaque necrosis [33]. For example, oxidized LDL has been shown to activate an ER stress–CHOP-induced cell death pathway through TLR2 or TLR4-mediated signaling in macrophages [33]. Recent studies have investigated evidence for a role for NOD1/NOD2 in the ER stress-induced inflammation via a peptidoglycan-independent mechanism [34]. In summary, in this study, we demonstrated a protective play of NOD2 during ER stress-induced VSMC death in processes related specifically to plaque necrosis. Our work will offer novel therapeutic targets, NOD2, for both the prevention and treatment of atherosclerosis.

Materials and methods

Animals

NOD2-deficient mice (NOD2^{-/-}) and ApoE-deficient mice (ApoE^{-/-}) were purchased from the Jackson laboratory (Bar Harbor, ME, USA) on a pure C57BL/6 genetic background, and NOD2 and ApoE double-deficient mice (NOD2^{-/-}ApoE^{-/-}) were generated by crossing NOD2^{-/-} with ApoE^{-/-} mice. These mice were maintained within the animal facilities at Harvard Medical School and University of Ulsan, in accordance with guidelines. All animal experiments were approved from the animal facilities (protocol 02773, UOU-2012-019).

Animal experiments and immunohistochemistry

The endoluminal injury to the mouse left common femoral artery was performed for femoral artery injury, and paraffin-embedded tissues were sectioned as described [35]. Vessel sections were stained using antibody against CHOP (Santa Cruz Biotechnology, CA) after femoral artery

injury. Seven- to 8-week-old male NOD2^{+/+}ApoE^{-/-} and NOD2^{-/-}ApoE^{-/-} mice were fed an atherogenic Paigen diet (Research Diets Inc., New Brunswick, NJ, USA) for 16 weeks before sacrifice. Necrotic core size was measured by calculating the percentage of the lesion that was acellular on hematoxylin and eosin (H&E) staining [36].

Plasma cholesterol, triglyceride, and free fatty acid measurements

At the time of sacrifice, plasma was collected via left ventricular puncture. Total plasma cholesterol (Invitrogen, Carlsbad, CA, USA), triglyceride (Asan Pharm. Co., LTD., Seoul, Korea), and free fatty acid (Biovision Inc., Milpitas, CA, USA) were measured using commercially available kits.

Cell culture and reagents

Primary wild-type (NOD2^{+/+}) and NOD2-deficient (NOD2^{-/-}) VSMCs from mice were isolated with the use of collagenase and elastase digestion of aortas, as described previously [37]. VSMCs were grown to ~80% confluence in DMEM media with 20% FBS. The VSMCs used were between passages 3 and 9. 293F cells were purchased from GIBCO (Life Technologies, Grand Island, NY, USA). Wild-type, XBP-deficient (XBP1^{-/-}), and ATF6-deficient (ATF6^{-/-}) MEFs (mouse embryonic fibroblasts) were kindly provided by SH Back. 293F cells and MEFs were cultured in DMEM (Life Technologies, Grand Island, NY, USA). Tunicamycin (Sigma-Aldrich, St Louis, MO, USA), Peptidoglycan (Sigma-Aldrich), iE-DAP (Invitrogen), MDP (Sigma-Aldrich), and other reagents (Sigma-Aldrich) were used.

Cell viability analysis

Cell viability was determined by MTS assay using the Cell-Titer 96® AQueous One Solution Cell Proliferation Assay kit (Promega, Madison, WI, USA) according to the manufacturer's protocol. Absorbance (490 nm) was then measured using a SpectraMax M2 microplate reader (Molecular Devices, San Jose, CA, USA) to calculate the cell viable percentages, and normalized by the control group.

Western blotting analysis and immunoprecipitation

Western blotting analysis was performed as previously described [38]. The membrane transferred samples were hybridized with antibodies, including CHOP, eIF2 α , phosphorylated eIF2 α , Bcl-xL, Bcl-2, Bak, GAPDH (Santa Cruz Biotechnology, Santa Cruz, CA), IRE1 α , caspase-3, cleaved caspase-3, PERK (Cell signaling, Boston, MA),

ATF4 (Proteintech Group Inc., Chicago, IL), ATF6 (IMGENEX, San Diego, CA), XBP1, phosphorylated IRE1 α (abcam®, Cambridge, MA, USA), KDEL (ENZO Life Sciences, Farmingdale, NY, USA), and β -actin (Sigma Chemicals, St Louis, MO, USA). Blots were then incubated with HRP-conjugated IgG and visualized with SuperSignal West Pico Chemiluminescent Substrate (Pierce, Rockford, IL, USA).

For immunoprecipitation, protein G Dynabeads (Invitrogen) was incubated with anti-FLAG antibody (Sigma Chemicals). Lysates were incubated with protein G Dynabeads (Invitrogen) and antibody. Beads were then rinsed and then resuspended in SDS/PAGE sample buffer.

Confocal microscopy

293F cells were grown on coverslips and were transfected with GFP-NOD2, RFP-PERK, RFP-IRE1, or RFP-ATF6. Cells were fixed in 4% formaldehyde. A nuclear was counterstained using a solution of Hoechst 33258 (Sigma-Aldrich) staining, and slide mounting was performed using Fluorescence Mounting Medium (Dako, Santa Clara, CA, USA). An Olympus FV1000 MPE microscope was used to acquire images.

Quantitative real-time RT-PCR

Total RNA was isolated using Trizol reagent (Invitrogen), and reverse transcription was performed using SuperScript™ III First-Strand Synthesis System (Invitrogen). The primer sequences were as follows: mouse CHOP forward (CTG CCT TTC ACC TTG GAG AC) and reverse (CGT TTC CTG GGG ATG AGA TA); mouse β -actin forward (CT CCA TCA TGA AGT GTG ACG) and reverse (ATA CTC CTG CTT GCT GAT CC).

Transfection and luciferase assays

Plasmids, pCGN/ATF6 (1–373), and pGL3/hCHOP (–870/+24) were provided by SH Back. pGL3/hCHOP (–160/+24) and pGL3/hCHOP (–79/+24) were cloned from pGL3/hCHOP (–870/+24) using restriction digestion. CHOP ERSE1/2 sites were changed from 5'-AATTC-3' to 5'-TGCCA-3', and CHOP ERSE1/2 minimal promoter constructs were cloned into the pGL2-promoter. Human CHOP promoter constructs [pGL3/hCHOP (–870/+24), pGL3/hCHOP (–665/+24), and pGL3/hCHOP (–160/+24)] were transfected with NOD2 or ATF6 expression plasmids, and pcDNA3/Flag-NOD2 or pCGN/ATF6 (1–373), respectively, in VSMCs. Mutations were introduced into the ERSE1/2 site sequence using an oligonucleotide with the sequence (–98) GCCGGCGAATTCCTTTCTGA (–79). CHOP ERSE1/2 (–98/–79) and ERSE1/2m minimal promoter constructs were cloned into the pGL2-promoter.

DNA transfection was performed using FuGENE6 transfection reagent (Roche, Indianapolis, IN, USA) according to the manufacturer's instructions. After 48 h incubation in fresh medium, cells were lysed in Reporter Lysis Buffer (Promega). To induce the CHOP promoter, cells were treated with tunicamycin for 18 h prior to harvesting. The cell lysates were used to determine luciferase activity using the Dual-luciferase® Reporter Assay System (Promega). Luciferase activity was normalized using beta-galactosidase.

Statistical analysis

Data are represented as mean \pm SD. For comparisons between two groups, we used a Student's two-tailed unpaired *t*-test. The Mann–Whitney *U*-test was performed to compare mRNA and protein expression. A statistically significant difference was indicated for $P < 0.05$.

Acknowledgements

It was supported by the basic science research program through the NRF, funded by the Ministry of Education (NRF-2014R1A6A1030318 to S.W.C.). It was supported by a grant from the KRIBB Research Initiative Program.

Conflicts of interest

The authors declare no conflict of interest.

Author contributions

MYK, SJL, and SWC designed experiments. MYK, NH, and SWC performed experiments. MYK, NH, SJL, MAP, and SWC analyzed data. SHB and MAP contributed new reagents and analytic tools; and SWC wrote the study.

References

- Lusis AJ (2000) Atherosclerosis. *Nature* **407**, 233–241.
- Clarke MC, Figg N, Maguire JJ, Davenport AP, Goddard M, Littlewood TD & Bennett MR (2006) Apoptosis of vascular smooth muscle cells induces features of plaque vulnerability in atherosclerosis. *Nat Med* **12**, 1075–1080.
- Clarke M & Bennett M (2006) The emerging role of vascular smooth muscle cell apoptosis in atherosclerosis and plaque stability. *Am J Nephrol* **26**, 531–535.
- Myoishi M, Hao H, Minamino T, Watanabe K, Nishihira K, Hatakeyama K, Asada Y, Okada K, Ishibashi-Ueda H, Gabbiani G *et al.* (2007) Increased endoplasmic reticulum stress in atherosclerotic plaques associated with acute coronary syndrome. *Circulation* **116**, 1226–1233.
- Chistiakov DA, Sobenin IA, Orekhov AN & Bobryshev YV (2014) Role of endoplasmic reticulum stress in atherosclerosis and diabetic macrovascular complications. *Biomed Res Int* **2014**, 1–14.
- Hu H, Tian M, Ding C & Yu S (2019) The C/EBP homologous protein (CHOP) transcription factor functions in endoplasmic reticulum stress-induced apoptosis and microbial infection. *Front Immunol* **9**, 1–50.
- Li Y, Guo Y, Tang J, Jiang J & Chen Z (2015) New insights into the roles of CHOP-induced apoptosis in ER stress. *Acta Biochim Biophys Sin* **2**, 146–147.
- Balamayooran T, Balamayooran G & Jeyaseelan S (2010) Toll-like receptors and NOD-like receptors in pulmonary antibacterial immunity. *Innate Immun* **16**, 201–210.
- Lauro ML, D'Ambrosio EA, Bahnson BJ & Grimes CL (2017) Molecular recognition of muramyl dipeptide occurs in the leucine-rich repeat domain of Nod2. *ACS Infect Dis* **3**, 264–270.
- Girardin SE, Boneca IG, Viala J, Chamaillard M, Labigne A, Thomas G, Philpott DJ & Sansonetti PJ (2003) Nod2 is a general sensor of peptidoglycan through muramyl dipeptide (MDP) detection. *J Biol Chem* **278**, 8869–8872.
- Oh HM, Lee HJ, Seo GS, Choi EY, Kweon SH, Chun CH, Han WC, Lee KM, Lee MS, Choi SC *et al.* (2005) Induction and localization of NOD2 protein in human endothelial cells. *Cell Immunol* **237**, 37–44.
- Davey MP, Martin TM, Planck SR, Lee J, Zamora D & Rosenbaum JT (2006) Human endothelial cells express NOD2/CARD15 and increase IL-6 secretion in response to muramyl dipeptide. *Microvasc Res* **71**, 103–107.
- Stroh T, Batra A, Glauben R, Bereswill S & Siegmund B (2008) NOD1 and 2: regulation of expression and function in preadipocytes. *J Immunol* **181**, 3620–3627.
- Ni G, Chen Y, Wu F, Zhu P & Song L (2017) NOD2 promotes cell proliferation and inflammatory response by mediating expression of TSLP in human airway smooth muscle cells. *Cell Immunol* **312**, 35–41.
- Kwon MY, Liu X, Lee SJ, Kang YH, Choi AM, Lee KU, Perrella MA & Chung SW (2011) Nucleotide-binding oligomerization domain protein 2 deficiency enhances neointimal formation in response to vascular injury. *Arterioscler Thromb Vasc Biol* **31**, 2441–2447.
- Thorp E, Li G, Seimon TA, Kuriakose G, Ron D & Tabas I (2009) Reduced apoptosis and plaque necrosis in advanced atherosclerotic lesions of Apoe^{-/-} and Ldlr^{-/-} mice lacking CHOP. *Cell Metab* **9**, 474–481.
- Ishiyama J, Taguchi R, Yamamoto A & Murakami K (2010) Palmitic acid enhances lectin-like oxidized LDL receptor (LOX-1) expression and promotes uptake of

- oxidized LDL in macrophage cells. *Atherosclerosis* **209**, 118–124.
- 18 Yoshida H, Okada T, Haze K, Yanagi H, Yura T, Negishi M & Mori K (2000) ATF6 activated by proteolysis binds in the presence of NF-Y (CBF) directly to the cis-acting element responsible for the mammalian unfolded protein response. *Mol Cell Biol* **20**, 6755–6767.
- 19 Brown BG, Zhao XQ, Sacco DE & Albers JJ (1993) Atherosclerosis regression, plaque disruption, and cardiovascular events: a rationale for lipid lowering in coronary artery disease. *Annu Rev Med* **44**, 365–376.
- 20 Frostegård J (2013) Immunity, atherosclerosis and cardiovascular disease. *BMC Med* **11**, 117.
- 21 Fredman G & Spite M (2013) Recent advances in the role of immunity in atherosclerosis. *Circ Res* **113**, e111–114.
- 22 Mehrhof FB, Schmidt-Ullrich R, Dietz R & Scheiderei C (2005) Regulation of vascular smooth muscle cell proliferation: role of NF-kappaB revisited. *Circ Res* **96**, 958–964.
- 23 Bennett MR, Sinha S & Owens GK (2016) Vascular smooth muscle cells in atherosclerosis. *Circ Res* **118**, 692–702.
- 24 Shanahan CM & Furmanik M (2017) Endoplasmic reticulum stress in arterial smooth muscle cells: a novel regulator of vascular disease. *Curr Cardiol Rev* **13**, 94–105.
- 25 Oyadomari S & Mori M (2004) Role of CHOP/GADD153 in endoplasmic reticulum stress. *Cell Death Differ* **11**, 381–389.
- 26 Tabas I (2010) The role of endoplasmic reticulum stress in the progression of atherosclerosis. *Circ Res* **107**, 839–850.
- 27 Park JS, Luethy JD, Wang MG, Fargnoli J, Fornace AJ Jr, McBride OW & Holbrook NJ (1992) Isolation, characterization and chromosomal localization of the human GADD153 gene. *Gene* **116**, 259–267.
- 28 Parkhouse R, Boyle JP, Mayle S, Sawmynaden K, Rittinger K & Monie TP (2014) Interaction between NOD2 and CARD9 involves the NOD2 NACHT and the linker region between the NOD2 CARDs and NACHT domain. *FEBS Lett* **588**, 2830–2836.
- 29 Negroni A, Pierdomenico M, Cucchiara S & Stronati L (2018) NOD2 and inflammation: current insights. *J Inflamm Res* **11**, 49–60.
- 30 Pellegrini E, Desfosses A, Wallmann A, Schulze WM, Rehbein K, Mas P, Signor L, Gaudon S, Zenkeviciute G, Hons M *et al.* (2018) RIP2 filament formation is required for NOD2 dependent NF-κB signalling. *Nat Commun* **9**, 4043.
- 31 Sorbara MT, Ellison LK, Ramjeet M, Travassos LH, Jones NL, Girardin SE & Philpott DJ (2013) The protein ATG16L1 suppresses inflammatory cytokines induced by the intracellular sensors Nod1 and Nod2 in an autophagy-independent manner. *Immunity* **39**, 858–873.
- 32 Zimmermann R, Eyrich S, Ahmad M & Helms V (2011) Protein translocation across the ER membrane. *Biochem Biophys Acta* **1808**, 912–924.
- 33 Zhao M, Pan W, Shi RZ, Bai YP, You BY, Zhang K, Fu QM, Schuchman EH, He XX & Zhang GG (2016) Acid sphingomyelinase mediates oxidized-LDL induced apoptosis in macrophage via endoplasmic reticulum stress. *J Atheroscler Thromb* **23**, 1111–1125.
- 34 Keestra-Gounder AM, Byndloss MX, Seyffert N, Young BM, Chávez-Arroyo A, Tsai AY, Cevallos SA, Winter MG, Pham OH, Tiffany CR & *et al.* (2016) NOD1 and NOD2 signalling links ER stress with inflammation. *Nature* **532**, 394–397.
- 35 Wei J, Gorman TE, Liu X, Ith B, Tseng X, Chen Z, Simon DI, Layne MD & Yet SF (2005) Increased neointima formation in CRP2-deficient mice in response to vascular injury. *Circ Res* **97**, 1323–1333.
- 36 Venegas-Pino DE, Banko N, Khan MI, Shi Y & Werstuck GH (2013) Quantitative analysis and characterization of atherosclerotic lesions in the murine aortic sinus. *J Vis Exp* **82**, 50933.
- 37 Hu Y, Zou Y, Dietrich H, Wick G & Xu Q (1999) Inhibition of neointima hyperplasia of mouse vein grafts by locally applied suramin. *Circulation* **100**, 861–868.
- 38 Chung SW, Chen YH & Perrella MA (2005) Role of Ets-2 in the regulation of HO-1 by endotoxin. *J Biol Chem* **280**, 4578–4588.